RSC Advances

ROYAL SOCIETY OF CHEMISTRY

www.rsc.org/advances

Highly dispersed Cu(II), Co(II) and Ni(II) catalysts covalently immobilized on imine modified silica for cyclohexane oxidation with hydrogen peroxide

R. Antony[a], S. Theodore David Manickam[a,*], Pratap Kollu[b], P.V. Chandrasekar[c],
K. Karuppasamy[a], S. Balakumar[a]

[a]Centre for Scientific and Applied Research, PSN College of Engineering and Technology, Tirunelveli-627 152, Tamil Nadu, India.

[b]Department of Metallurgical Engineering and Materials Science, Indian Institute of Technology, Mumbai-400076, India.

[c]College of Physics and Information Engineering, Institute of Optoelectronic Display, Fuzhou University, Fuzhou-350002, PR China.

Abstract

This paper describes the synthesis of Cu(II), Co(II) and Ni(II) catalysts immobilized on imine functionalized silica gel through 3-aminopropyltriethoxysilane linker. The synthesized catalysts were characterized by spectroscopic techniques namely EDS, FT-IR, UV-Vis., ^{29}Si MAS NMR, powder XRD and ESR spectroscopy. These analytical methods evidently confirmed the formation of silica supported catalysts. Thermal properties of catalysts were studied between 30-800 °C by thermo gravimetric-differential thermo gravimetric (TG-DTG) analysis. The surface roughness of silica gel was increased upon modifications, but without losing its lumpy shape as evidenced by SEM investigation. Magnified SEM and AFM images together suggested the high dispersive nature of catalysts. Cyclohexane was successfully converted into cyclohexanol and cyclohexanone by the catalysts with an aid of hydrogen peroxide (oxidant). Comparatively, Cu(II) catalyst exhibited better cyclohexane conversion than other catalysts. The reusable nature of the catalysts was established by performing five consecutive catalytic run with Cu(II) catalyst. Comparatively, the present reported catalytic systems would be the simple, reusable and effective models for higher cyclohexane conversion with better product selectivity.

Keywords: silica gel; Schiff base; heterogeneous catalysts; ESR spectroscopy; cyclohexane;

*Corresponding author (S. Theodore David Manickam). E-mail: s.theodore.david@gmail.com

1. Introduction

Oxidation of organic substrates containing inert C-H bonds is one of the desirable and challenging organic transformation[1, 2] for researchers. Specifically, oxidation of C-H bond available in cyclohexane is an important area in synthetic chemistry as there is an upward attention on using its products such as cyclohexanol and cyclohexanone (also known KA oil). For example, its products are employed as starting materials for the manufacture of adipic acid, polyamide-6, acidulant in baking powder and caprolactam. Appreciably, caprolactam is an important precursor in the manufacture of commercial products like nylon-6 and nylon-6,6'[3, 4]. The current existing industrial procedure involves 150 °C temperature and 1-2 MPa pressure over metal cobalt salt or metal-boric acid catalyst for just 4% conversion of cyclohexane into cyclohexanol and cyclohexanone. Besides, this commercial technique yields more cyclohexanol and some additional steps are required to get better cyclohexanol/cyclohexanone ratio[5, 6]. Due to these limitations, the search of new catalysts for the effective oxidation of cyclohexane has become imperative. In this exploration, heterogeneous catalysts are often preferred over homogeneous catalysts due to easy catalyst separation, excellent reusability and chemical and thermal stability[7, 8]. These outstanding qualities build heterogeneous catalysts as environmentally benign catalysts. Different types of heterogeneous catalysts have been endeavoured for cyclohexane oxidation and few instances are Co(II) and Cr(VI) on poly(4-vinylpyridine-co-divinylbenzene) (4.64% conversion)[9]; scorpionate Fe(III) complex on carbon materials (20.8% conversion)[10] and desilicated MOR zeolite (37.2% conversion)[11] in the presence of co-catalyst and co-oxidant; and gold nanoparticles on carbon materials (3.6% conversion)[12]. In spite of that, silica gel is relatively more desirable support than aforementioned supports due to its low price, excellent stabilities, good accessibilities and organic groups can be robustly anchored to the surface of the silica gels[13, 14]. With these salient features, silica supported catalysts have exposed superior cyclohexane conversion too. Few examples are listed here. Urus et al have achieved 99.99% cyclohexane conversion with silica supported complexes. But they employed microwave irradiation and attained very poor cyclohexanol and cyclohexanone selectivity[15]. Mesoporous silica materials such as MCM-41 (45.5% conversion with 51.9% cyclohexanol and 48.1% cyclohexanone selectivity)[16] and SBA-15 (71.1% conversion with 26% cyclohexanol and 74% cyclohexanone selectivity)[17] have also been strived for better cyclohexane conversion. But tedious procedures, exercising more chemicals and relatively high cost are necessitated in the synthesis of mesoporous silica materials. In this circumstance, aforesaid demerits would suppress the utility of effective silica supported catalysts. Therefore, it is important to find simple, low cost and effective silica supported catalysts for cyclohexane oxidation with enhanced selectivity.

In the drive towards the preparation of heterogeneous catalysts using silica materials, various approaches have been followed. Among them, incorporation of organic entity (flexible spacer) onto silica is considered as the best one. The major benefit in anchoring organic groups onto silica is the easier formation of catalytic centre[18, 19]. The method of organo-modification of inorganic materials is usually divided into two classes. In class I, organic and inorganic components are embedded and only hydrogen, van der Walls or ionic bonds provide cohesion to the whole structure. Whereas in class II, the two phases (organic and inorganic) are linked together through strong chemical covalent or coordinative bonds[20-22]. The class II type is more favoured than class I, since it affords an additional chemical strength to the organo-modified inorganic materials. Furthermore, covalent immobilization of metal complexes to the solid support offers high catalytic efficiency and better recyclability without having the inherent problems like leaching of complex/ligand during the reaction[23, 24]. Silica based materials have been frequently organo-modified by class II method using 3-aminopropyltriethoxysilane (APTES) as the linker between silica materials and the organic entity[22, 25, 26]. This linker compound may go through the formation of Schiff base ligands on the route to organo-modification of silica. The added applications with forming Schiff bases are their chelating ability with transition metal ions, stability under variety of oxidative and reductive conditions and borderline nature between hard and soft Lewis bases. As well, when Schiff base ligands are administered as their metal complexes, the range of their applications has been enhanced[27, 28]. Isatin is the most reported endogenous indole due to its reaction with primary amines for the preparation of Schiff bases[29, 30].

Based on the above facts, here we aspire to accomplish the new recyclable silica supported catalytic systems with sufficient catalytic ability and selectivity under environmentally tolerable conditions for cyclohexane oxidation. New silica supported Cu(II), Co(II) and Ni(II) catalysts (catalysts 1, 2 and 3, respectively), derived through 3-amino modification and imine functionalization of silica gel, have been synthesised and applied in catalytic cyclohexane oxidation using hydrogen peroxide as oxidant. The reason for using hydrogen peroxide is its environmental benign character as it decomposes to give only water and oxygen. Thus using hydrogen peroxide is always safe and promising approach for a variety of oxidation reactions[31]. This work also comprises characterization of catalysts using EDS, FT-IR, UV-Vis., ^{29}Si NMR, powder XRD and ESR; surface studies (SEM and AFM); and thermal study (TG-DTG).

2. Experimental

2.1. Materials

3-aminopropyl triethoxysilane (APTES) was procured from Himedia. Silica gel, metal salts, isatin, cyclohexane, acetonitrile, toluene and hydrogen peroxide were purchased from E-Merck. All the chemicals and solvents were employed without further purification.

2.2. Synthesis of amino modified silica gel (SiO_2-NH_2)

50 gm silica gel was pre-treated by refluxing with excess amount of 1:1 hydrochloric acid for 6 h. It was filtered off and washed with sufficient amount of deionised water till the pH becomes 7. The resultant product was dried at 120 °C for 12 h. Then, 20 g pre-treated silica was taken in 100 ml toluene followed by the addition of 20 ml APTES and the resultant

mixture was refluxed for 72 h. The final suspension was filtered off, washed with excess amount of toluene, ethanol and diethyl ether and dried at 100 °C under vacuum.

2.3. Synthesis of imine modified silica gel (L)

For the preparation of L, 5 mmol isatin and 5 gm SiO_2-NH_2 were taken in 100 ml deionised water. The ensuing mixture was then magnetically stirred for 24 h at 60 °C in the reaction flask. The obtained brown colour solid product was filtered, washed repeatedly with water and dried at 100 °C.

2.4. Synthesis of catalysts

2 gm L and 50 ml deionised water were mixed in the reaction flask towards the synthesis of catalyst 1. To this mixture, 5 mmol copper chloride was added and magnetically stirred at ambient temperature for 24 h. The achieved product was filtered and washed thoroughly with water and dried at 90 °C under vacuum. Likewise, catalysts 2 and 3 were synthesised from their corresponding metal chlorides. The schematic manifestation for the synthesis of catalysts is shown in Fig. 1.

2.5. Characterization

FT-IR spectra were recorded on a Jasco FT-IR 4100 spectrophotometer from KBr pellets containing 1% of the sample in 4000-400 cm^{-1} wave number region with 2 cm^{-1} resolution. Electronic spectral studies were performed on a Shimadzu UV-2600 spectrophotometer in 200-800 nm wavelength range using diffuse reflectance (DR) technique. ^{29}Si cross polarized magic angle spinning nuclear magnetic resonance (^{29}Si CP MAS NMR) spectral analysis of L and catalyst 1 was achieved on Mercury Plus 300 MHz NMR spectrometer (VARIAN, USA) equipped with a 5 mm dual broad band probe. Thermal properties of the compounds were investigated by TG-DTG technique using a Mettler Toledo star system under dynamic N_2 atmosphere within 30-800 °C temperature range at a heating rate of 10 °C min^{-1}. Powder X-ray diffraction (PXRD) determinations were executed on X-ray diffractometer ((XPERT PRO PANalytical, Netherland)) for phase identification. The patterns were run with CuKα radiation with a secondary monochromator (λ= 0.1545 nm) at 40 kV and 30 mA. The morphologies, dimensions and elemental compositions of catalysts were explored using a scanning electron microscope of Hitachi S-3400N model attached with energy dispersive spectroscope. The SEM images were taken at 15 kV accelerating voltage with 2 kX magnification range under liquid N_2 atmosphere. For studying particle distribution, the AFM analysis was accomplished on catalyst 1 using AFM XE 70, park systems.

2.6. Oxidation of cyclohexane

The oxidation reactions were carried out in the 25 ml flask equipped with magnetic stirrer. The flask was charged with 0.05 g of the catalyst (1/2/3) in 10 ml acetonitrile. Then, 10 mmol of 30% H_2O_2 solution and 5 mmol of cyclohexane were added successively. This reaction mixture was stirred in the reaction flask at 70 °C under atmospheric pressure conditions for 12 h. Aliquots from the reaction mixture were taken at the time intervals of 2 h for product analysis to examine the effect of reaction time on cyclohexane conversion percentage. Two other separate catalytic experiments (one without catalyst and another without oxidant) were also performed by using similar reaction procedure. The product samples were investigated using Hewlett–Packard gas chromatograph (HP 6890) having FID detector, a capillary column (HP-5), a programmed oven with temperature range from 50 to 200 °C and N_2 carrier gas at a flow rate of 0.5 $cm^3 min^{-1}$. The conversion percentage of cyclohexane and selectivity for cyclohexanol and/or cyclohexanone was calculated using the equations given below:

$$\text{Conversion \% of cyclohexane} = 100 \times [\text{Initial \%} - \text{Final \%}] / \text{Initial \%}$$

$$\text{Selectivity (\%)} = 100 \times [\text{GC Peak area \% of cyclohexanol and/or cyclohexanone}] / \sum \text{Peak area of total products}.$$

3. Results and discussion

3.1. Characterization of catalysts

The presence of expected elements in the respective prepared compounds is confirmed by EDS analysis. The EDS spectra of silica gel, SiO_2-NH_2, L and the catalysts (1, 2 and 3) are illustrated in supplementary file (ESI). The formation of catalysts is identified by the indicative peaks of corresponding metal ions in their EDS spectra.

The FT-IR spectra of silica gel, SiO_2-NH_2 and L are compared and shown in Fig. 2. In the FT-IR spectrum of silica gel (Fig. 2a), the bands at 3548 (broad) and 1632 cm^{-1} are assigned to the stretching and bending vibrations of silanol groups (Si-OH), respectively. The bands found at 1094 and 798 cm^{-1} are the characteristic anti-symmetric and symmetric stretching modes (Si-O-Si) of $[SiO_4]$ units, respectively. A small shoulder observed at 974 cm^{-1} can be allocated to the Si-OH stretching mode and band at 462 cm^{-1} is the evidence of Si-O-Si bending vibrations[32, 33]. As shown in Fig. 2b, the appearance of new continuing band in the region of 3290-3000 cm^{-1}, characteristic stretching vibration of NH_2 group, confirms the aminopropylation of silica support. It is further supported by the stretching and bending vibration modes of aliphatic CH_2 groups, appeared at 2938 and 1495 cm^{-1}, respectively. The NH_2 bending vibration of SiO_2-NH_2 emerges at 1572 cm^{-1}. In the FT-IR spectrum of L (Fig. 2c), stretching and bending vibrations of $–NH_2$ group are disappeared due to the imine (C=N) group formation by the reaction of isatin with SiO_2-NH_2. The occurrence of this reaction is also proved by the presence of new characteristic bands at 1714 and 1629 cm^{-1} which are the indicative peaks for stretching modes of C=O and C=N groups, respectively. In addition to these changes, the new band is found at 1467 cm^{-1} because of aromatic –C=C- stretch. The anticipated amide –NH stretch is masked by the broad Si-OH stretching vibration. In the FT-IR spectra of catalysts, it is expected that coordination of nitrogen centre to the metal ion would reduce the electron density in the imine link and shift the C=N stretching frequency to the lower wave numbers. In Fig. 3, the downward shift in C=N stretch is found in all catalysts, which implies the successful coordination of azomethine nitrogen to the metal centre[34]. Furthermore, the C=O group of L is also be expected to coordinate with the metal ion through its oxygen atom and it is confirmed by the shift in their stretching frequency to the lower region. The evident stretching bands for M-N and M-O may be superimposed with the sharp

Si-O-Si bending vibration modes noted at 460 cm^{-1}. Besides, the existence of characteristic bands of silica support in the FT-IR spectra of SiO_2-NH_2, L and all catalysts, show that the fundamental structure of the parent silica support could not be disturbed even after the organo-modification and catalysts' formation.

UV-Vis. spectroscopy is the best selection to assign the geometry of the metal complexes around the metal centre. The DR UV-Vis. spectra of L and catalysts are illustrated in Fig. 4 while the same for silica gel and SiO_2-NH_2 are presented in supplementary file (ESI). In general, for the aromatic ring containing Schiff base ligands, two types of electronic transitions are suspected (π-π* and n-π* transitions). The UV-Vis. spectrum of L (Fig. 4a) displays two such characteristic absorption bands below 400 nm. The band at 220 nm is due to π-π* transition (characteristic of π-bonds of aromatic ring, C=N and C=O groups). Another expected band at 340 nm is assigned to n-π* transition, characteristic of non-bonded electrons available on nitrogen (C=N) and oxygen (C=O).

The UV-Vis. spectra of catalysts 1 and 2 reveal similar pattern, however they are found to be different from that of the catalyst 3. As found in UV-Vis. spectrum of L, characteristic bands for π-π* and n-π* transitions at around 220 and 340 nm, respectively are discovered in UV-Vis. spectra of catalysts also. A new band at 450 nm can be attributed to the ligand to metal charge transfer (LMCT). It suggests the coordination of L with the metal ions. This coordination behaviour of L is further endorsed by the appearance of new significant d-d transition band of the metal ions. Catalyst 1 shows a broad band centred at 600 nm which might be attributed to d-d transition of Cu(II) (Fig. 4b). The d-d transitions with very close energy may overlap together and lead into the emergence of very broad single d-d band. Similarly, catalyst 2 shows the d-d transition as a broad band centred at 600 nm (Fig. 4c). For catalyst 3, this characteristic d-d band is perceived at 520 nm (Fig. 4d) and it is not much broad like catalysts 1 and 2. The entry of this characteristic d-d transition band in UV-Vis. spectra of all the catalysts confirms the FT-IR investigation to assure the formation of catalysts and suggesting an approximate square planar geometry[35-37].

The changes in the silicon environment of silica gel after modification have been studied by ^{29}Si CP MAS NMR technique. For the unmodified silica gel, the anticipated characteristic peaks are regularly appeared at ~110, ~105 and ~90 ppm which can be allocated to ($(SiO)_4Si$) silica sites, ($(SiO)_3SiOH$) terminal silanol sites and ($(SiO)_2Si(OH)_2$) geminal silanol groups, respectively. Among them, the peak at 110 ppm is predominant owing to the abundance of ($(SiO)_4Si$) silica sites[38-41]. Fig. 5a and 5b show ^{29}Si NMR spectra of L and catalyst 1, respectively. In these spectra, the intense peak at 109 ppm, corresponds to ((($(SiO)_4Si$))) silica sites. In contrast, the other two expected peaks are less intense. Importantly, in the ^{29}Si NMR spectra of both L and catalyst 1, an additional broad peak is seen at ~60 ppm owing to the formation of new of ($(SiO)_3SiC$) sites[42]. These observations are indications of the covalent modification of silica gel backbone through the reaction between terminal and geminal surface silanol groups. Though these peaks are found in ^{29}Si NMR spectra of both L and catalyst 1, their position and intensity are slightly unequal which may be due to the consequence of Cu(II) coordination with L.

The wide angle PXRD patterns of unmodified silica gel, SiO_2-NH_2 and all catalysts are shown in Fig. 6. The obtained patterns of all the compounds display a similar broad band centred at 22° as the substantiation to amorphous nature and topological structure of SiO_2 support[38, 43, 44]. On comparison with unmodified silica gel (Fig. 6a), the intensity of this characteristic peak, in PXRD patterns of all modified silica gels, is found to be decreased along with line broadening. This decrease in intensity is perhaps assigned to the filling of pores of silica surface by metal ions or reduction in X-ray scattering contrast between the channel wall of silicate frame work and L. Furthermore, no new peaks are acquired after amino modification, imine modification and catalysts' formation. It can be ascribed that the amorphous nature of silica is maintained even after modification reactions. However, this amorphous nature is not maintained in case of catalyst 1 as evidenced by the new peaks appeared in Fig. 6d, which means that the crystallinity of L gets enhanced after metallation with Cu(II) ions.

ESR spectra of catalysts 1 and 2 (given in Fig. 7a and 7b, respectively) were recorded at 77 K temperature and employed to verify the geometry around central metal ions of the catalysts. The resultant spectra are found to be typical for axial nature and the detected *g* factors are in the order of $g_{\parallel} > g_{\perp} > 2.0023$ for both the catalysts. In case of catalyst 1, this order indicates that the unpaired electron most probably dwells in the $d_x{}^2$-$d_y{}^2$ orbital and it is likely to be square planar geometry as conferred in UV-Vis. spectroscopy[45]. The $g_{\parallel}$ value seems to be less than 2.3 and it is a clear indication for the covalent character of Cu-L bond as suggested by Kivelson and Niemon[46]. The exchange coupling factor (G) can be expressed by the subsequent equation:

$$G = (g_{\parallel}-2) / (g_{\perp}-2)$$

As reported earlier, for the parallely aligned or slightly misaligned local axes, the G value is greater than 4.0 whereas it is less than 4.0 for appreciably misaligned local axes with considerable exchange coupling. From the ESR spectrum of catalyst 1, the calculated G value is 7.0 and hence only the negligible exchange coupling could be possible[47, 48]. On the other side, catalyst 2 displays a very broadened ESR spectrum, perhaps due to differences in the relaxation parameters and the spin-spin interaction between Co(II) ions[49].

Fig. 8 depicts the TG-DTG patterns of L and all the catalysts studied. In Fig. 8a, L exhibits three mass loss stages correspond to desorption of physically adsorbed water molecules (0-110 °C), decay of organic contents (160-370 °C) and dehydroxylation of surface silanol groups (370-700 °C). Similar thermal decomposition steps are observed also in TG-DTG curves of all the catalysts (Fig. 8b-8d). But the calculated % weight loss values are not comparable as in the case of L and most probably it is due to the coordination of metal ions with L. Significantly and contrary to L, metal complexes exhibit a new weight gain step above

600 °C. This may be the characteristic for the formation of metal oxides through oxidation reactions. The TG-DTG studies also support the formation of catalysts from L. The details of weight loss and weight gain values are separately presented as a table in supplementary file (ESI).

In order to find out the difference between the size and surface morphology of SiO_2-NH_2 and its modified forms (L and catalysts), SEM study has been employed. The SEM photographs are given in Fig. 9. For comparison, SEM photograph of unmodified silica gel is given in supplementary file (ESI). Silica gel display clear surface and there is no evidence for the presence of any adsorbed particles in its surface. After modification with APTES, the surface shows the presence of adsorbed particles as seen in SEM image of SiO_2-NH_2 (Fig. 9a). The number of particles in the surface is found to be enhanced upon organo-modification of SiO_2-NH_2 with isatin for the formation of L. This noteworthy change in surface (Fig. 9b) can further confirm the formation of L. In general, the modification of porous silica gel with organic functionalities may assist the effective adsorption of metal ions[50, 51]. In fact, as evidenced by the SEM images of catalysts, the metal ions are adsorbed via complex formation throughout the surface of L in a dispersed manner. To confirm the dispersion of metal ions, the magnified SEM image of catalyst 1 is also illustrated in Fig. 9f. This uniform metal ions' scattering on to L perhaps provide the greater surface area for the better catalytic activity of catalysts. Throughout the modification process, silica gel particles do not lose their lumpy shape.

Fig. 10 demonstrates the 2D and 3D AFM images of catalyst 1 in two different magnifications for the further investigation of surface properties, and particularly particles dispersion. From the AFM images, it is obvious that the particles are found to be emerged as the cone shaped heaps. They are not agglomerated and well strewn with each other. These observations supplement the surface information obtained from the SEM images.

3.2. Catalytic study

Owing to the commercial advantages of cyclohexane oxidation, it has been selected as the model reaction to study the catalytic properties of catalysts 1, 2 and 3. As it leaves only water as the by-product, H_2O_2 was employed as oxidant. According to Corma et al, the role of solvent in the catalytic reactions is sometimes crucial as it develops different phases into uniform and thus upholding mass transportation. The solvents can affect the intermediate species which further alter the reaction mechanism and also take part in tuning the surface properties of catalysts and reaction path-ways[52]. By comparison, acetonitrile was found to be the effective solvent than others as evidenced by the literature[17, 53]. Hence, in this study also the catalytic cyclohexane oxidation was performed in acetonitrile.

Catalyst 1/2/3 catalysed oxidation of cyclohexane mainly yields cyclohexanone and cyclohexanol. In gas chromatograph analysis also, there is no evidence for other products. After the completion of catalytic reactions, acid-base titration was also carried out with the product mixture to check the formation of acidic product (adipic acid). On cooling the product mixture, no white precipitate was developed. This observation and acid-base titration results suggested that no adipic acid was formed. So the general pictorial representation of cyclohexane oxidation to cyclohexanol and cyclohexanone is made as in Fig. 11.

3.2.1. Effect of temperature

When the cyclohexane oxidation was attempted at room temperature (25 °C), only negligible cyclohexane conversion was obtained. Therefore, the reaction temperature was raised stepwise to find the optimum reaction temperature. Upon increasing the reaction temperature, the cyclohexane conversion efficiency was increased up to 70 °C irrespective of the catalyst. Further increase of temperature after 70 °C could not show any significant change in the cyclohexane conversion. This may be due to the fact that 70 °C is closer to the boiling point of cyclohexane. Consequently, 70 °C was fixed as the most favourable temperature to supply adequate energy to cross over the energy barrier of cyclohexane oxidation reaction. The catalytic activity of catalysts 1, 2 and 3 at different temperature between 30 to 80 °C is given in Fig. 12. Reaction temperature has shown meaningful effect only on cyclohexane conversion % and no such effect detected on product selectivity.

3.2.2. Effect of reaction time

The catalytic activity of all catalysts was independently studied in cyclohexane oxidation for 12 h. In order to explore the effect of reaction time on cyclohexane conversion efficiency, the aliquots from the reaction media were taken out between the time intervals of 2 h. The cyclohexane conversion efficiency exhibited by all catalysts at the time intervals of 2 h is provided in Table 1. All the complexes showed increase in catalytic activity with the increase of time. However, further increase of time after 12 h could not show any improved conversion efficiency. Unlike reaction temperature, reaction time has considerably changed both cyclohexane conversion % and product selectivity. In particular, the notable observation from the time dependant catalytic study of catalysts is that the cyclohexanone selectivity increased with the increase of reaction time irrespective of all the complexes. On the other hand, the cyclohexanol selectivity has been found to decrease with the increase of reaction time. This confirms that cyclohexane is first oxidized into cyclohexanol and subsequently to cyclohexanone.

Catalyst 1 showed better catalytic efficiency compared to catalysts 2 and 3. In detail, it demonstrates 49% cyclohexane conversion at 12 h, with 27% cyclohexanol and 73% cyclohexanone product selectivity. Catalysts 2 and 3 also revealed comparatively adequate cyclohexane conversion (40 and 37%, respectively). The higher catalytic efficiency of catalyst 1 can be attributed to its effectiveness in decomposing hydrogen peroxide. Though the catalytic efficacy of catalysts 2 and 3 is similar, catalyst 2 yielded better cyclohexanone selectivity (14% cyclohexanol & 86% cyclohexanone). The variation in product selectivity may be due to the nature of the metal ions in the catalysts. The coordinatively unsaturated metal ion species such as Co(II), Ni(II) and Cu(II) present in their corresponding catalysts play a crucial role on promoting the catalytic performance. The adequate catalytic activity of all the studied catalysts (1, 2 and 3) may be due to their coordination with the dispersed pre-installed imine sites of imine modified silica gel (L). Two blank experiments were also accomplished separately, one without oxidant and another any without catalyst but kept other conditions unchanged. The obtained product yield was very meagre. It supports the role of catalysts (metal ion species) in cyclohexane oxidation reaction as very extensive.

3.2.3. Catalytic recyclability

The salient feature of supported complex catalyst is their stability in the successive catalytic run. To study the stability of the catalysts, catalyst 1 was opted as it showed superior catalytic activity than other two catalysts. The catalyst 1 was filtered off after the first catalytic run, washed with ethanol and ether, and re-employed in the next catalytic run. The reusability of catalyst was explored by carrying out five consecutive catalytic run by maintaining all other conditions unaltered.

The results of this reusability study are illustrated in Fig. 13. Cyclohexane conversion efficiency of the catalyst has been seemed to be well comparable throughout the catalytic cycle. Comprehensively, the catalyst lost only 3% of its original catalytic activity at fifth catalytic run and selectivity of the products was also comparable in each catalytic run. It proves the excellent stability of catalysts covalently immobilized on silica gel. This catalytic study suggests that no copper ion has been leached out of the surface of silica gel inside the catalytic solution. This is also being suggestive of the stability of silica supported complex. Further, the FT-IR spectra of the fresh catalyst and the used catalyst were compared and both of them were found to be similar. These experiments substantiate that the reported catalysts are heterogeneous in nature due to the silica support afforded *via* covalent approach.

In comparison, the silica supported catalysts depict superior catalytic performance in cyclohexane conversion than our previously reported corresponding chitosan supported catalysts[54]. Perhaps it could be due to the well dispersed surface of silica supported catalysts than that of chitosan supported analogues. Also these silica supported catalysts are proved to have better recyclability than corresponding chitosan supported catalysts.

4. Conclusion

In summary, Cu(II), Co(II) and Ni(II) catalysts derived by coordination reaction with imine modified silica gel were proved to be highly dispersed as deliberated by SEM and AFM studies. This high dispersive nature of reported catalysts forced us to apply them in cyclohexane oxidation using hydrogen peroxide oxidant. The formation of catalysts was confirmed by spectral techniques such as EDS, FT-IR, DR UV-Vis., PXRD and ^{29}Si CP MAS NMR have been employed to explore the structure of ligand (L) and catalysts, and they successfully confirmed their formation. UV-Vis. and ESR spectroscopic methods together suggested the square planar geometry to the catalysts irrespective of metal ions. The weight gain noticed in TG-DTG curves of the catalysts further confirmed the coordination of metal ions to silica support. Among the catalysts studied, Cu(II) catalyst (catalyst 1) displayed superior catalytic behaviour (49% cyclohexane conversion) than other two catalysts. However, in terms of selectivity, Co(II) catalyst (catalyst 2) is proposed as the better catalyst as it yielded 86% cyclohexanone. Regardless of catalysts, the increase of reaction time leads to higher cyclohexanone selectivity due to the subsequent oxidation of cyclohexanol. The reported covalently silica supported catalysts were established as stable, simple, inexpensive, easily prepared and best heterogeneous catalysts as they maintained their original catalytic behaviour for repeated catalytic runs. Therefore, in green approach, these catalysts may open a new avenue for cyclohexane oxidation with hydrogen peroxide.

Acknowledgement

STDM expresses his gratitude for financial aid (Sanction No: (2010/34/8/BRNS/772) sanctioned by Department of Atomic Energy-Board of Research in Nuclear Sciences (DAE-BRNS), Government of India, Mumbai to carry out this work. RA thanks DAE-BRNS for the financial support in the form of Junior and Senior Research Fellowships. PK acknowledges Department of Science and Technology (DST) for DST-INSPIRE faculty fellowship and Sophisticated Analytical and Instrumentation Facility, Indian Institute of Technology Bombay, Mumbai, India for helping with characterization facilities. All the authors are deeply grateful to Mr. K. Saravanan, CSIR-CSMCRI, Bhavnagar, India for his valuable contribution in discussing the catalytic results.

References

1. A. E. Shilov and G. B. Shul'pin, *Chem. Rev.*, 1997, **97**, 2879-2932.
2. R. Sheldon, *Metal-catalyzed oxidations of organic compounds: mechanistic principles and synthetic methodology including biochemical processes*, Elsevier, 2012.
3. R. Zhao, D. Ji, G. Lv, G. Qian, L. Yan, X. Wang and J. Suo, *Chem. Commun.*, 2004, 904-905.
4. N. V. Maksimchuk, K. A. Kovalenko, V. P. Fedin and O. A. Kholdeeva, *Chem. Commun.*, 2012, **48**, 6812-6814.
5. T. F. Silva, G. S. Mishra, M. F. G. da Silva, R. Wanke, L. M. Martins and A. J. Pombeiro, *Dalton Trans.*, 2009, 9207-9215.
6. R. Whyman, *Applied organometallic chemistry and catalysis*, Oxford University Press, 2001.
7. C. González-Arellano, A. Corma, M. Iglesias and F. Sánchez, *Adv. Synth. Catal.*, 2004, **346**, 1316-1328.
8. M. B. Gawande, P. S. Branco and R. S. Varma, *Chem. Soc. Rev.*, 2013, **42**, 3371-3393.
9. D. Lončarević, J. Krstić, J. Dostanić, D. Manojlović, Ž. Čupić and D. Jovanović, *Chem. Eng. J.*, 2010, **157**, 181-188.
10. L. Martins, M. P. de Almeida, S. Carabineiro, J. Figueiredo and A. Pombeiro, *ChemCatChem*, 2013, **5**, 3847-3856.

11. L. Martins, A. Martins, E. Alegria, A. Carvalho and A. Pombeiro, *Appl. Catal. A*, 2013, **464**, 43-50.
12. S. Carabineiro, L. Martins, M. Avalos-Borja, J. Buijnsters, A. Pombeiro and J. Figueiredo, *Appl. Catal. A*, 2013, **467**, 279-290.
13. G. Fink, B. Steinmetz, J. Zechlin, C. Przybyla and B. Tesche, *Chem. Rev.*, 2000, **100**, 1377-1390.
14. H. Guo, X. Liu, Q. Xie, L. Wang, D.-L. Peng, P. S. Branco and M. B. Gawande, *RSC Advances*, 2013, **3**, 19812-19815.
15. S. Uruş, M. Dolaz and M. Tümer, *J. Inorg. Organomet. Polym.*, 2010, **20**, 706-713.
16. J. Zhao, W. Wang and Y. Zhang, *J. Inorg. Organomet. Polym.*, 2008, **18**, 441-447.
17. S. Alavi, H. Hosseini-Monfared and M. Siczek, *J. Mol. Catal. A*, 2013, **377**, 16-28.
18. P. T. Tanev, M. Chibwe and T. J. Pinnavaia, *Nature*, 1994, **386**, 321.
19. A. Stein, B. J. Melde and R. C. Schroden, *Adv. Mater.*, 2000, **12**, 1403-1419.
20. S. Attia, A. Shames, I. Zilbermann, G. Goobes, E. Maimon and D. Meyerstein, *Dalton Trans.*, 2014, **43**, 103-110.
21. C. Freire, C. Pereira and S. Rebelo, *Catalysis*, 2012, **24**, 116.
22. F. Hoffmann, M. Cornelius, J. Morell and M. Fröba, *Angew. Chem. Int. Ed.*, 2006, **45**, 3216-3251.
23. C. E. Song and S.-g. Lee, *Chem. Rev.*, 2002, **102**, 3495-3524.
24. A. Corma and H. Garcia, *Adv. Synth. Catal.*, 2006, **348**, 1391-1412.
25. J. P. Reynhardt, Y. Yang, A. Sayari and H. Alper, *Chem. Mater.*, 2004, **16**, 4095-4102.
26. A. Schätz, M. Hager and O. Reiser, *Adv. Funct. Mater.*, 2009, **19**, 2109-2115.
27. A. K. Singh, V. Gupta and B. Gupta, *Anal. Chim. Acta*, 2007, **585**, 171-178.
28. S. Chang, L. Jones, C. Wang, L. M. Henling and R. H. Grubbs, *Organometallics*, 1998, **17**, 3460-3465.

29. M. A. Ali, H. J. Hj Abu Bakar, A. Mirza, S. Smith, L. Gahan and P. V. Bernhardt, *Polyhedron*, 2008, **27**, 71-79.

30. G. F. Caramori, R. L. Parreira and A. M. D. C. Ferreira, *Int. J. Quantum Chem.*, 2012, **112**, 625-646.

31. J. M. Campos-Martin, G. Blanco-Brieva and J. L. Fierro, *Angew. Chem. Int. Ed.*, 2006, **45**, 6962-6984.

32. G. Dıaz, R. Perez-Hernandez, A. Gomez-Cortes, M. Benaissa, R. Mariscal and J. Fierro, *J. Catal.*, 1999, **187**, 1-14.

33. Z. Huang, F. Cui, H. Kang, J. Chen, X. Zhang and C. Xia, *Chem. Mater.*, 2008, **20**, 5090-5099.

34. S. Jana, B. Dutta, R. Bera and S. Koner, *Langmuir*, 2007, **23**, 2492-2496.

35. W.-J. Zhou, B. Albela, P. Perriat, M.-Y. He and L. Bonneviot, *Langmuir*, 2010, **26**, 13493-13501.

36. C. Brückner, V. Karunaratne, S. J. Rettig and D. Dolphin, *Can. J. Chem*, 1996, **74**, 2182-2193.

37. F. Feigl, *Chemistry of specific, selective and sensitive reactions*, Academic Press, 1949.

38. P. Yin, Y. Tian, Z. Wang, R. Qu, X. Liu, Q. Xu and Q. Tang, *Mater. Chem. Phys.*, 2011, **129**, 168-175.

39. C. Pereira, J. F. Silva, A. M. Pereira, J. P. Araújo, G. Blanco, J. M. Pintado and C. Freire, *Catal. Sci. Tech.*, 2011, **1**, 784-793.

40. T. Yokoi, H. Yoshitake, T. Yamada, Y. Kubota and T. Tatsumi, *J. Mater. Chem.*, 2006, **16**, 1125-1135.

41. M. A. B. Meador, E. F. Fabrizio, F. Ilhan, A. Dass, G. Zhang, P. Vassilaras, J. C. Johnston and N. Leventis, *Chem. Mater.*, 2005, **17**, 1085-1098.

42. X. Wang, G. Wu, W. Wei and Y. Sun, *Catal. Lett.*, 2010, **136**, 96-105.

43. N. An, W. Zhang, X. Yuan, B. Pan, G. Liu, M. Jia, W. Yan and W. Zhang, *Chem. Eng. J.*, 2013, **215**, 1-6.

44. J. Wang, J. Sun, Y. Li and F. Wang, *Luminescence*, 2013.

45. S. Deshpande, D. Srinivas and P. Ratnasamy, *J. Catal.*, 1999, **188**, 261-269.

46. D. Kivelson and R. Neiman, *J. Chem. Phys.*, 2004, **35**, 149-155.

47. B. Hathaway and D. Billing, *Coord. Chem. Rev.*, 1970, **5**, 143-207.

48. R. Dudley and B. Hathaway, *J. Chem. Soc. A*, 1970, 1725-1728.

49. J. Evans, A. Zaki, M. El-Sheikh and S. El-Safty, *J. Phys. Chem. B*, 2000, **104**, 10271-10281.

50. S. Uruş, S. Purtaş, G. Ceyhan and T. Erkenez, *Sep. Purif. Technol.*, 2013, **118**, 432-447.

51. S. Uruş, S. Purtaş, G. Ceyhan and F. Tümer, *Chem. Eng. J.*, 2013, **220**, 420-430.

52. A. Corma, M. Camblor, P. Esteve, A. Martinez and J. Perezpariente, *J. Catal.*, 1994, **145**, 151-158.

53. C. K. Modi and P. M. Trivedi, *Arabian J. Chem.*, 2013.

54. R. Antony, S. Theodore David, K. Saravanan, K. Karuppasamy and S. Balakumar, *Spectrochim. Acta A*, 2013, **103**, 423-430.

Figure Captions

Fig. 1 Schematic showing the synthetic route of imine modified silica gel (L) and catalysts

Fig. 2 FT-IR spectra of silica gel (a), amino modified silica gel, SiO_2-NH_2 (b) and imine modified silica gel, L (c)

Fig. 3 FT-IR spectra of imine modified silica gel, L (a) and catalysts *viz* 1 (b), 2 (c) and 3 (d)

Fig. 4 DR UV-Vis. spectra of imine modified silica gel, L (a) and catalysts *viz* 1 (b), 2 (c) and 3 (d)

Fig. 5 ^{29}Si CP MAS NMR spectra of imine modified silica gel, L (a) and catalyst 1 (b)

Fig. 6 XRD patterns of silica gel (a), amino modified silica gel, SiO_2-NH_2 (b), imine modified silica gel, L (c) and catalysts *viz* 1 (d), 2 (e) and 3 (f)

Fig. 7 ESR spectra of catalyst 1 (a) and catalyst 2 (b)

Fig. 8 TG-DTG patterns of imine modified silica gel, L (a) and catalysts *viz* 1 (b), 2 (c) and 3 (d)

Fig. 9 SEM photographs of amino modified silica gel, SiO_2-NH_2 (a), imine modified silica gel, L (b) and catalysts *viz* 1 (c), 2 (d) and 3 (e). Magnified SEM image of catalyst 1 (f)

Fig. 10 2D (a) and 3D (b) AFM images (10X10 μm); 2D (c) and 3D (d) AFM images (2.5X2.5 μm) of catalyst 1

Fig. 11 Schematic showing catalytic cyclohexane oxidation into cyclohexanol and cyclohexanone

Fig. 12 Effect of temperature on cyclohexane oxidation catalysed by Cu(II), Co(II) and Ni(II) catalysts containing imine modified silica gel, L

Fig. 13 Recyclability of catalyst 1. Reaction conditions: cyclohexane 5 mmol, 10 mmol 30% H_2O_2, 0.05 g catalyst, 10 ml CH_3CN, 70 °C and 12 h

Table Captions

Table 1 Product yield and selectivity % in cyclohexane oxidation catalysed by Cu(II), Co(II) and Ni(II) catalysts containing imine modified silica gel, L

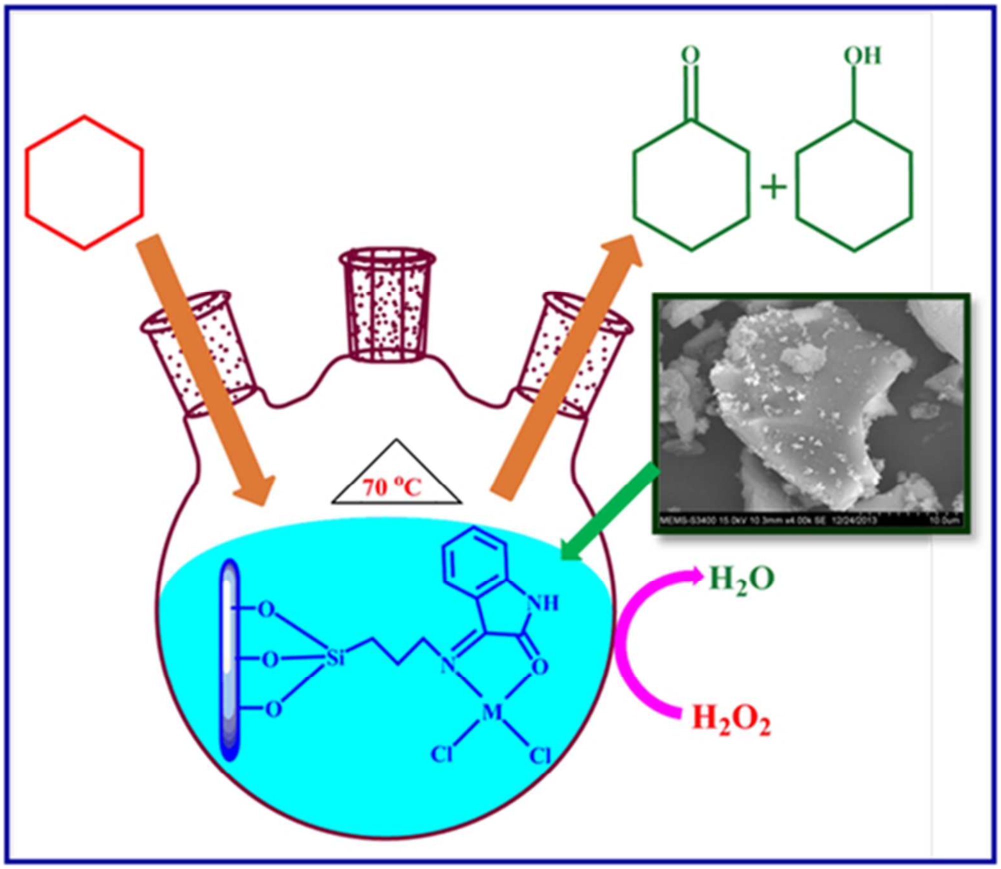

157x135mm (96 x 96 DPI)

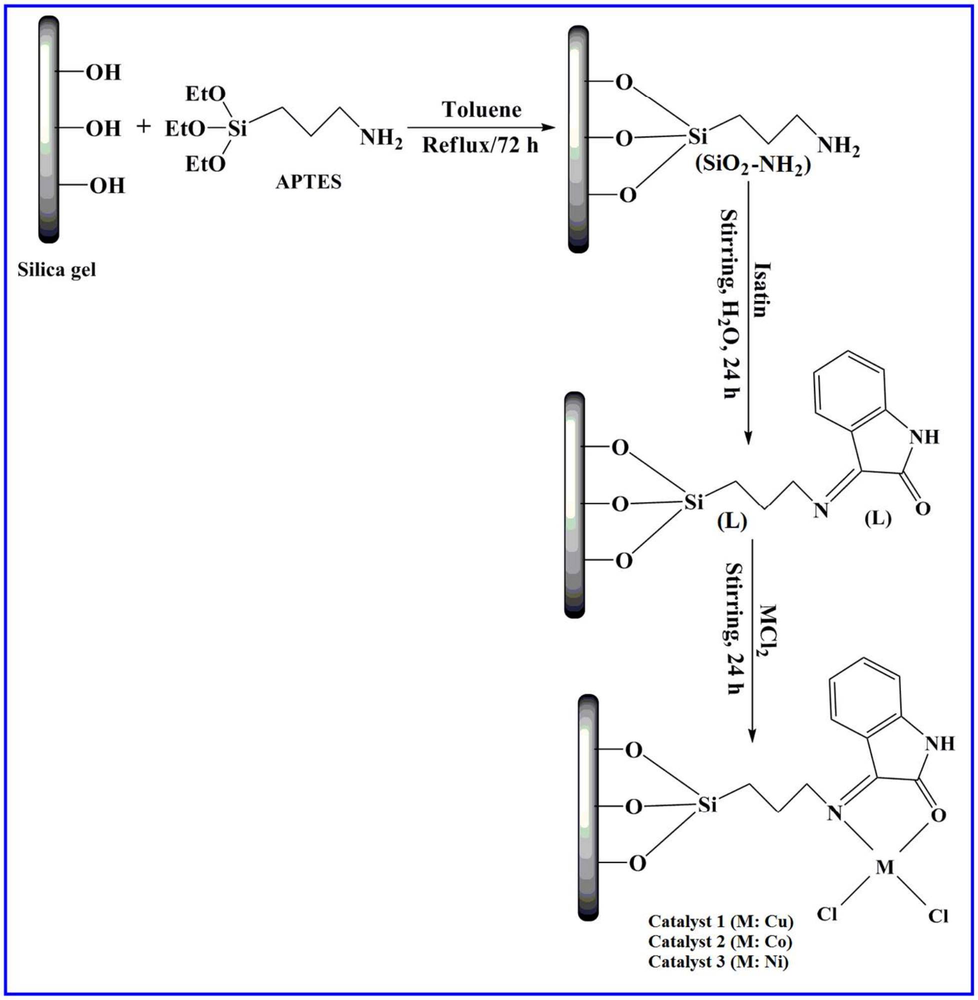

Schematic showing the synthetic route of imine modified silica gel (L) and catalysts
135x137mm (300 x 300 DPI)

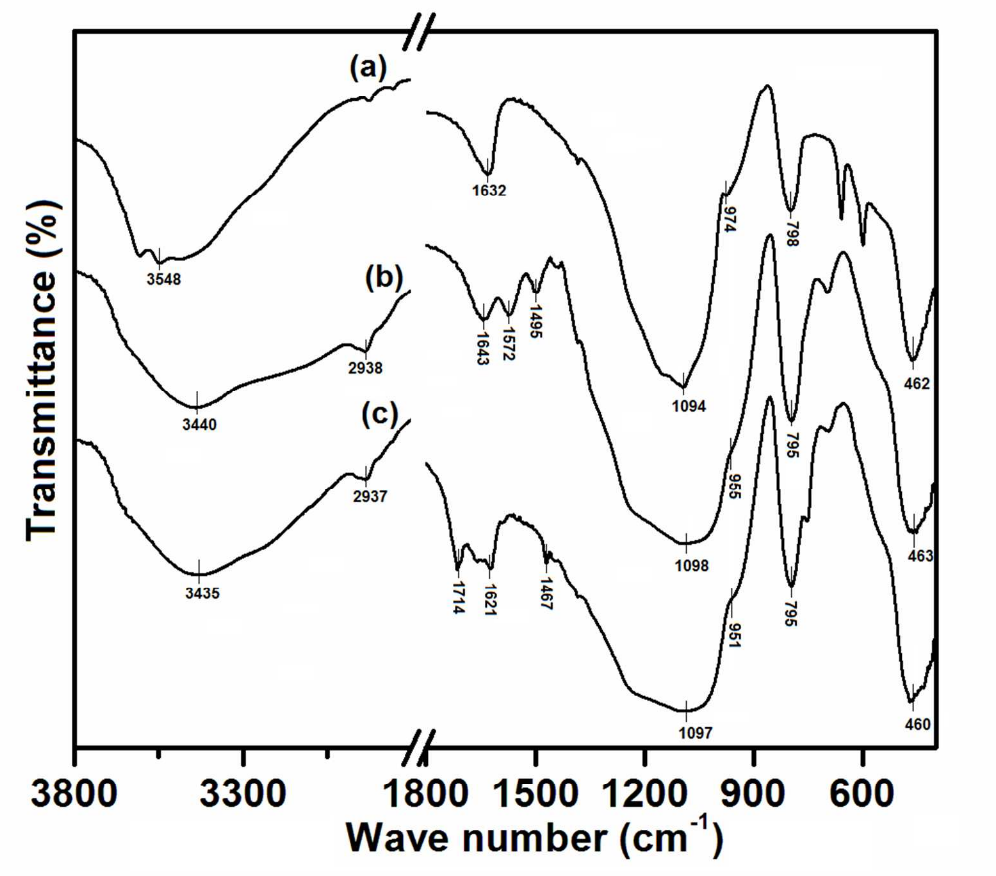

FT-IR spectra of silica gel (a), amino modified silica gel, SiO2-NH2 (b) and imine modified silica gel, L (c)
274x242mm (96 x 96 DPI)

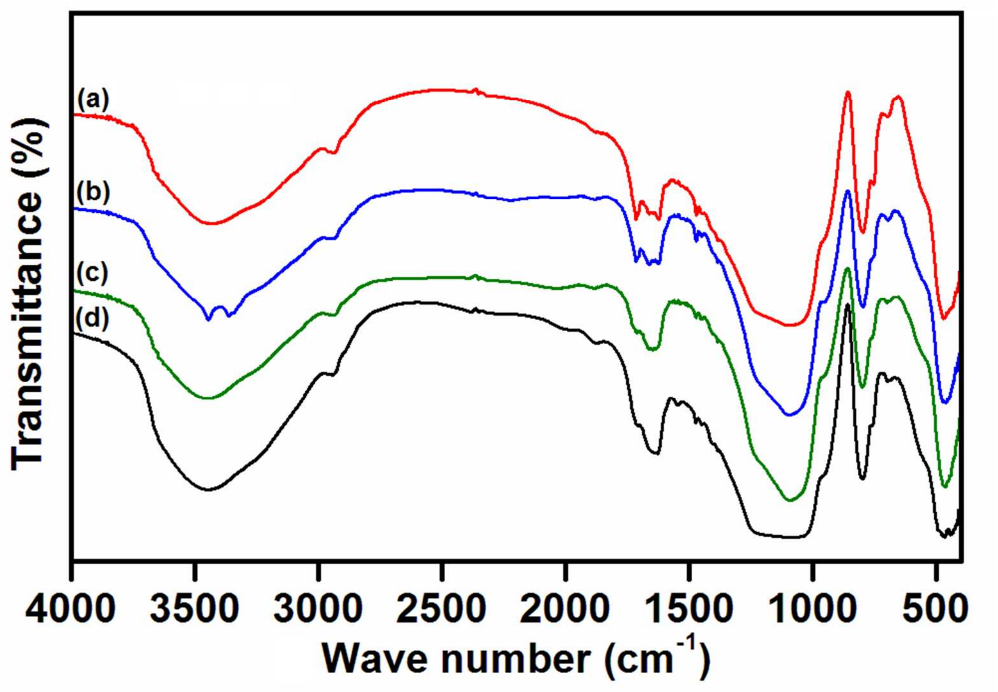

FT-IR spectra of imine modified silica gel, L (a) and catalysts viz 1 (b), 2 (c) and 3 (d)
169x117mm (150 x 150 DPI)

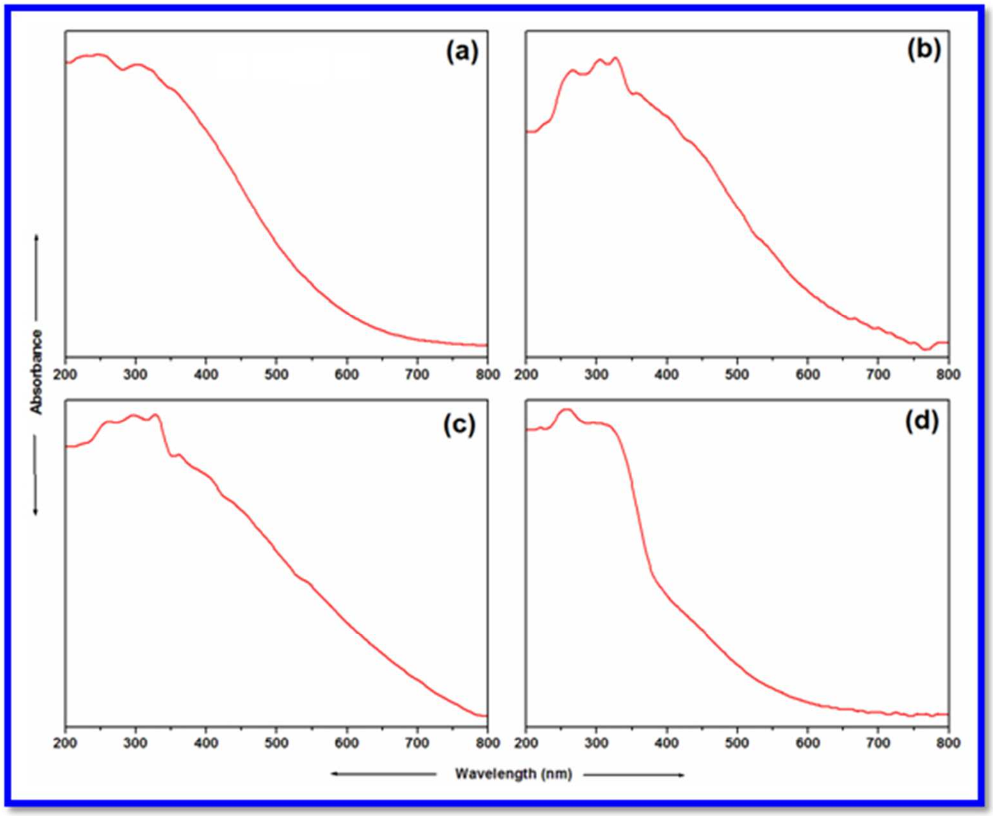

DR UV-Vis. spectra of imine modified silica gel, L (a) and catalysts viz 1 (b), 2 (c) and 3 (d)
155x132mm (96 x 96 DPI)

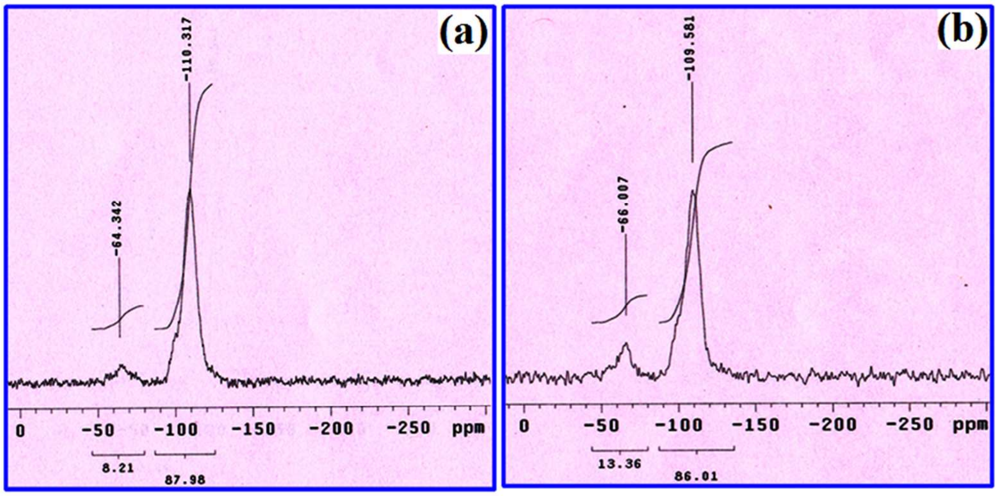

29Si CP MAS NMR spectra of imine modified silica gel, L (a) and catalyst 1 (b)
229x116mm (96 x 96 DPI)

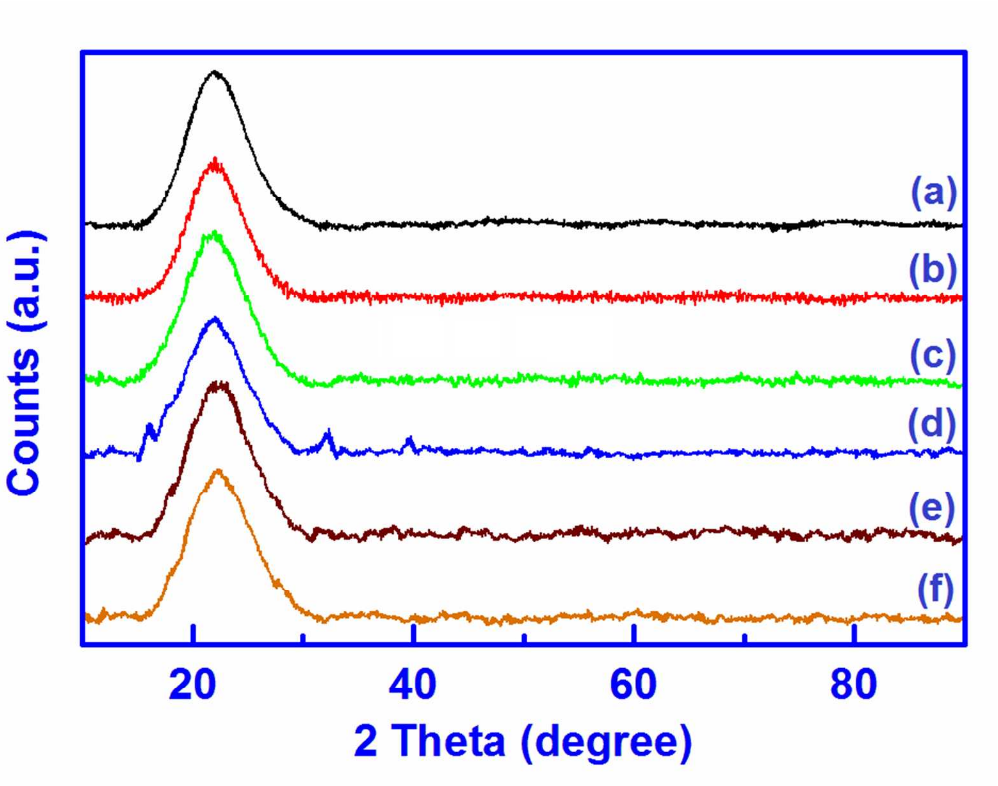

XRD patterns of silica gel (a), amino modified silica gel, SiO2-NH2 (b), imine modified silica gel, L (c) and catalysts viz 1 (d), 2 (e) and 3 (f)
158x124mm (150 x 150 DPI)

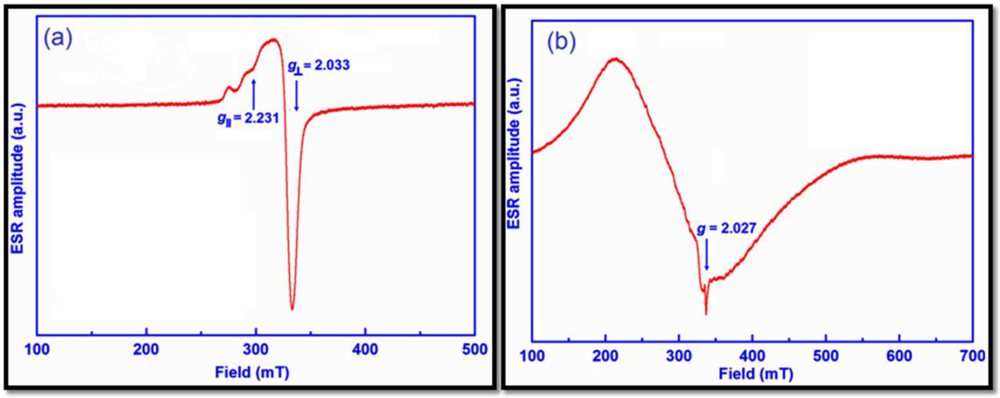

ESR spectra of catalyst 1 (a) and catalyst 2 (b)
238x96mm (96 x 96 DPI)

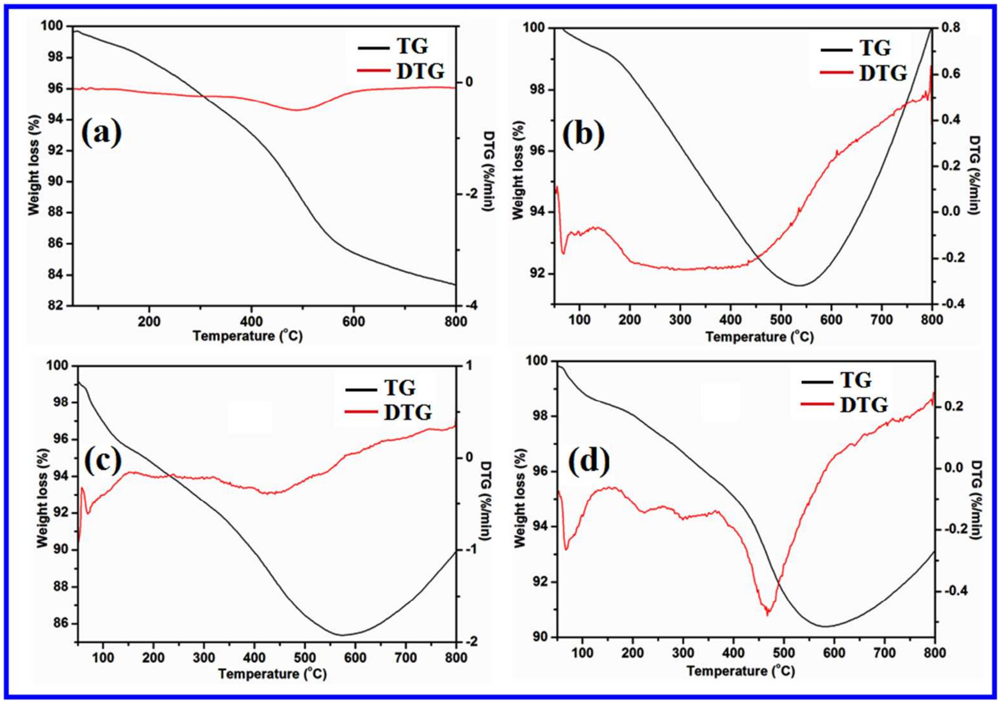

TG-DTG patterns of imine modified silica gel, L (a) and catalysts viz 1 (b), 2 (c) and 3 (d)
275x192mm (96 x 96 DPI)

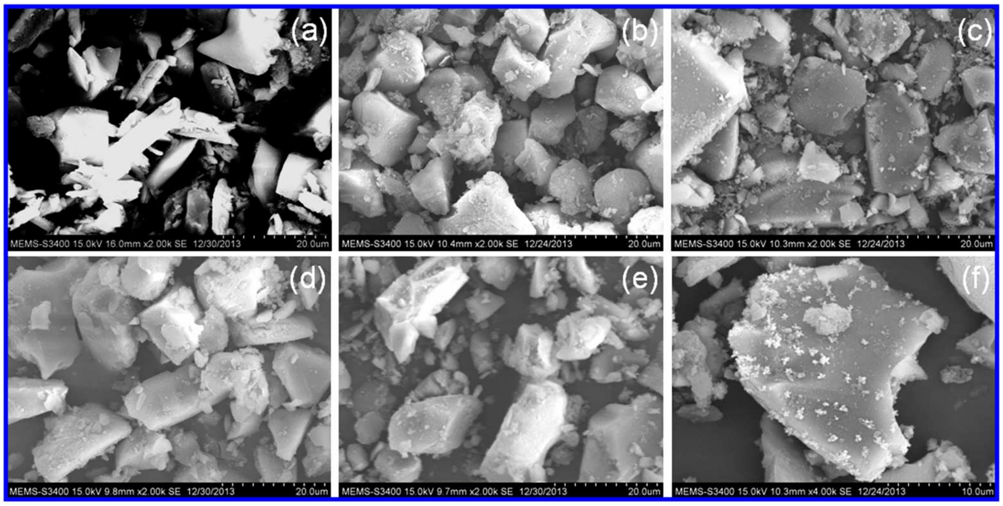

SEM photographs of amino modified silica gel, SiO2-NH2 (a), imine modified silica gel, L (b) and catalysts viz 1 (c), 2 (d) and 3 (e). Magnified SEM image of catalyst 1 (f)
308x155mm (96 x 96 DPI)

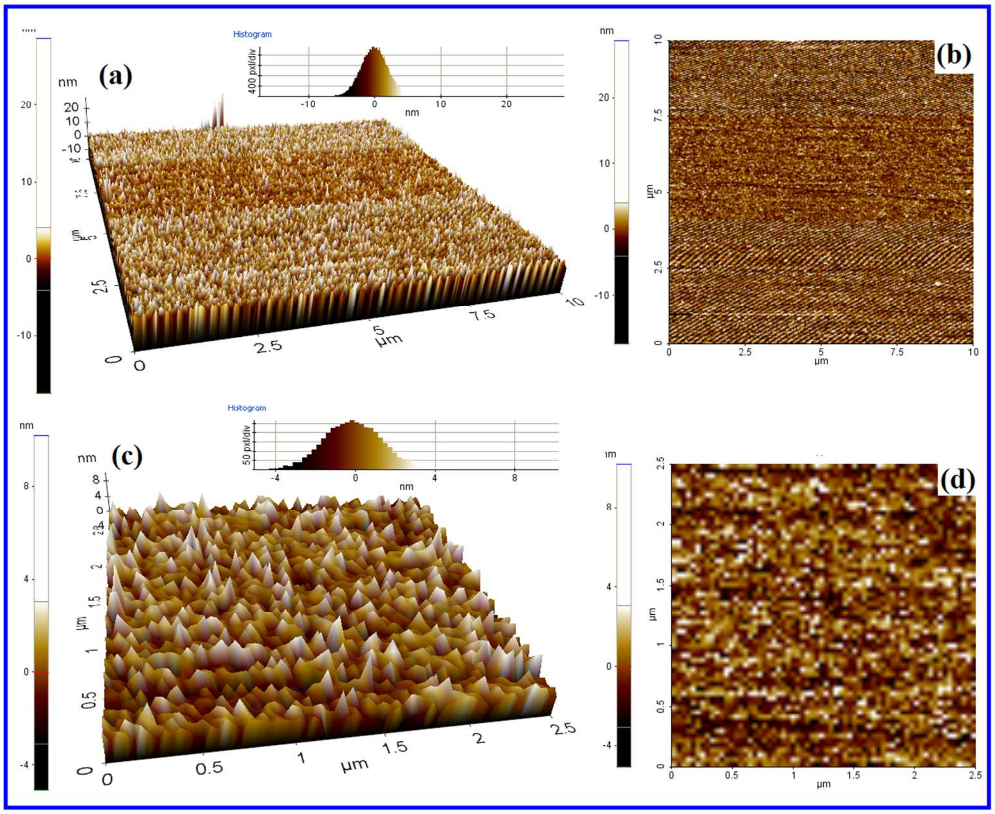

2D (a) and 3D (b) AFM images (10X10 µm); 2D (c) and 3D (d) AFM images (2.5X2.5 µm) of catalyst 1
334x273mm (96 x 96 DPI)

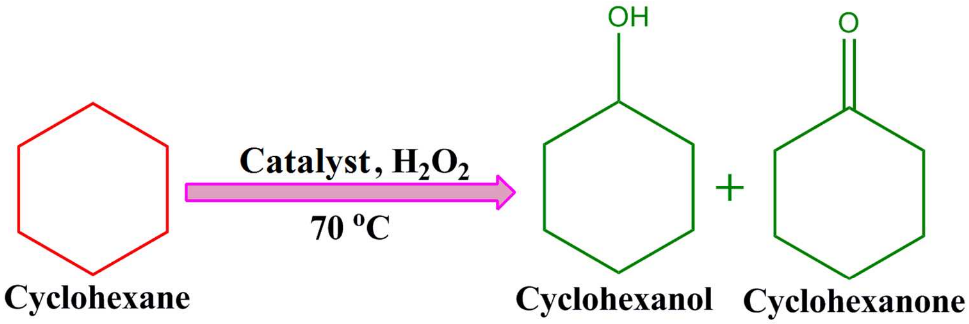

Schematic showing catalytic cyclohexane oxidation into cyclohexanol and cyclohexanone
385x142mm (96 x 96 DPI)

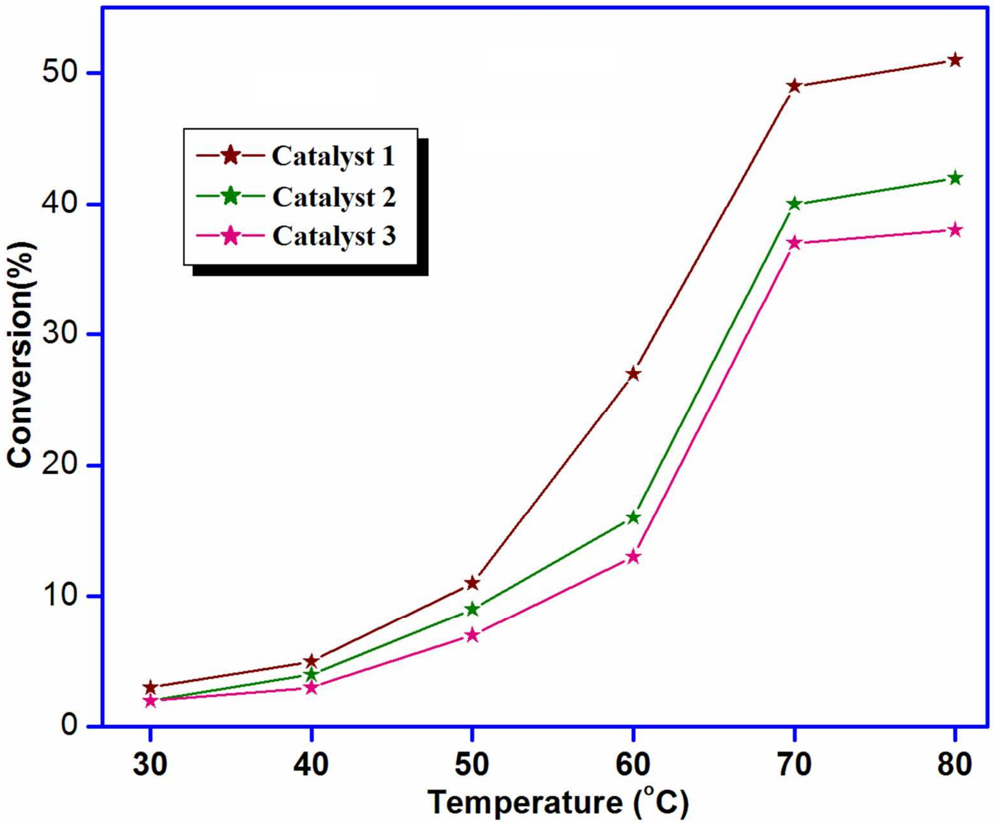

Effect of temperature on cyclohexane oxidation catalysed by Cu(II), Co(II) and Ni(II) catalysts containing imine modified silica gel, L
215x176mm (150 x 150 DPI)

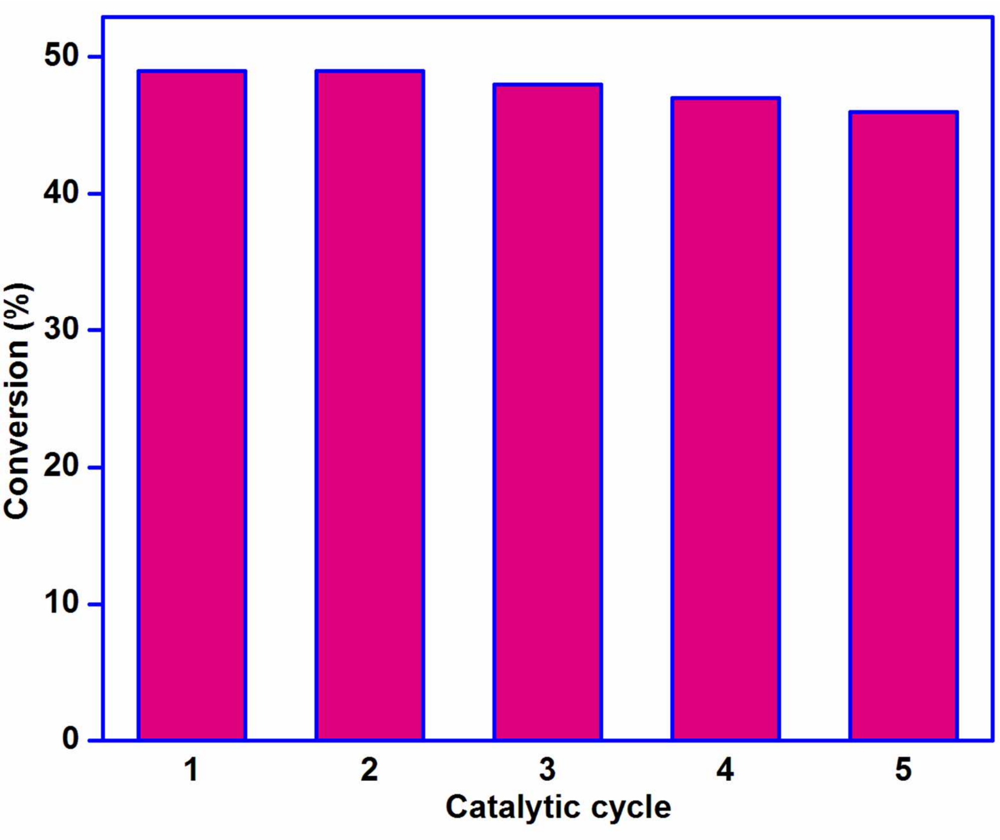

Recyclability of catalyst 1. Reaction conditions: cyclohexane 5 mmol, 10 mmol 30% H2O2, 0.05 g catalyst, 10 ml CH3CN, 70 °C and 12 h
214x180mm (150 x 150 DPI)

Catalyst	Time (h)	Conversion (%)	Selectivity (%)	
			Cyclohexanol	Cyclohexanone
1	2	8	71	29
	4	16	62	38
	6	30	50	50
	8	41	41	59
	10	46	35	65
	12	49	27	73
2	2	6	67	33
	4	13	54	46
	6	24	45	55
	8	33	31	69
	10	39	22	78
	12	40	14	86
3	2	5	69	31
	4	11	59	41
	6	20	52	48
	8	31	40	60
	10	35	28	72
	12	37	21	79

Reaction conditions: cyclohexane 5 mmol, 10 mmol 30% H_2O_2, 0.05 g catalyst, 10 ml CH_3CN and 70 °C